Histone deacetylase inhibitor quisinostat activates caspase signaling and upregulates p53 acetylation to inhibit the proliferation of HepG2 cells

FENGSHAN LI, TIEGONG WANG, ZHENYONG WANG, XIONGFEI CHEN and RUHAI LIU

First Department of General Surgery, Cangzhou Central Hospital, Cangzhou, Hebei 061001, P.R. China

Received February 27, 2017; Accepted August 3, 2017

DOI: 10.3892/mmr.2017.7355

Abstract. Histone deacetylase inhibitor (HDACi) has been a major target of anticancer agents. Quisinostat (JNJ-26481585), a novel second-generation HDACi, has previously demonstrated antiproliferative activity against non-small cell lung cancer; however, the function of quisinostat in hepatocellular carcinoma (HCC) remains to be elucidated. In the present study, it was revealed that quisinostat suppressed the cell viability of HepG2 cells *in vitro* and *in vivo*. Increased cell apoptosis was observed in quisinostat-treated HepG2 cells. The underlying mechanism revealed that quisinostat treatment activates the cleavage of caspase proteins. Furthermore, quisinostat upregulated p53 acetylation at K381/K382 sites by impairing the interaction between histone deacetylase 6 and p53, which resulted in the activation of p53, and triggered cell cycle arrest at the G_1 phase. Collectively, the results of the present study demonstrated the antiproliferative effect of quisinostat on HepG2 cells; these results suggest that histone deacetylase may be a promising therapeutic target of HCC.

Introduction

Hepatocellular carcinoma (HCC) is a common type of the primary malignancy of liver cancer, which is the third leading cause of cancer-related deaths worldwide (1). The incidence of HCC is increasing in both developing countries and economically developed regions (2,3). A variety of risk factors are contributed to the development of HCC, including chronic liver inflammation caused by hepatitis B and C infection, obesity (4), diabetes-induced liver fibrosis and the environmental factors (5-7). Currently, surgical resection and liver transplant have been the two major therapeutic options in the treatment of liver cancer (6). Nevertheless, since patients are most often diagnosed at the advantaged stage with tumor metastasis, surgery is only favorable for about 20% of liver cancer cases. For patients harboring cancer metastasis, chemotherapy has been one of the most important methods used in clinical practice, however, with the more concern on the side-effect and resistance, the amplification of chemotherapy in cancer is limited (8). Therefore, developing new strategies for liver cancer treatment requires further investigation.

Increasing evidence has suggested that epigenetic changes are involved in the development and progression of malignant cancers (9-12). The acetylation modification of histone is generally considered as the most extensively studied epigenetic event (13), which is regulated by histone acetyltransferases (HATs) and histone deacetylases (HDACs) (14). HDACs are overexpressed in a variety of cancers and correlated with the poor prognosis of cancer patients (15-18). Currently, histone deacetylase inhibitors (HDACi) are a major focus of accumulating interests as anticancer agents, which function through blocking histone deacetylation and modifying chromatin structure and gene expression (17,19,20). In addition to histone, a wide range of non-histone proteins are also modified by acetylation and regulated by HDACi. Quisinostat (JNJ-26481585), a novel second-generation HDACi, has high specificity toward class I and II HDACs (21,22). Quisinostat has shown anti-proliferative activity against non-small cell lung cancer (NSCLC) (22), however, the therapeutic effect of quisinostat on HCC remains largely unknown.

In this study, we investigated the effect of quisinostat on the cell growth of HCC. Our results showed that HCC cells exposed to quisinostat treatment exhibited decreased cell viability. Quisinostat treatment increased the acetylation of p53 and induced cell cycle arrest and cell apoptosis. Our results provide insights into the potential use for quisinostat as a novel chemotherapeutic agent in HCC treatment.

Materials and methods

Cell culture. HCC cell line HepG2 (harboring wild-type p53 (23,24)) was purchased from the Cell Bank of the Chinese Academy of Sciences (Shanghai, China). Cells were cultured in RPMI-1640 medium (GIBCO, Grand Island, NY, USA) containing 10% fetal bovine serum at 37˚C in a 5% CO_2 incubator and passaged once every 2-3 days.

Correspondence to: Professor Ruhai Liu, First Department of General Surgery, Cangzhou Central Hospital, Cangzhou, Hebei 061001, P.R. China
E-mail: liu_ruhai@yeah.net

Key words: hepatocellular carcinoma, quisinostat, caspase, p53 acetylation, cell apoptosis

Cell viability assay. The cell viability assay was performed using the Cell Counting Kit-8 (CCK-8) (Beyotime Institute of Biotechnology, Shanghai, China) according to the manufacturer's instructions. Briefly, HepG2 cells were cultured in the 96-plates with the cell density at $1x10^3$ per well. Cells were exposed to the indicated concentration of quisinostat (dissolved in DMSO as stock solutions and kept at room temperature) at different time point. And then medium was removed, 10 μl of CCK-8 and 100 μl of serum free medium were added. Cells were incubated at 37˚C for 1 h. The absorbance of each well was measured at 450 nm using the microplate reader (Thermo Fisher Scientific, Waltham, MA, USA). The experiment was performed in triplicate.

Cell apoptosis analysis. Cell apoptosis assay was performed with the Annexin V-FITC Apoptosis Detection kit (Invitrogen, Carlsbad, CA, USA) according to the protocol of manufacturer. HepG2 cells pretreated with quisinostat were trypsinized and washed with pre-cold PBS. The samples were centrifuged for 5 min at 400 x g. Discard the supernatant and suspend the cells with 1x Annexin-binding buffer with a final density of ~$1x10^6$ cells/ml. Cells were then stained with Annexin V-fluorescein isothiocyanate (FITC) and PI working solution for 15 min in the darkness at room temperature. The cell apoptosis rate was analyzed using flow cytometry.

In vitro colony formation assay. Five hundred HepG2 cells were seeded into the 6-well plate and cultured for 7 days. And then the culture medium was replaced with fresh medium containing quisinostat with the indicated concentration and cultured for another 7 days. The colony formation of HepG2 cells was stained with 0.05% crystal violet for 5 min at room temperature.

Western blot analysis. Cells with the indicated treatment were harvested and lyzed with NP-40 lysis buffer. The protein concentration was determined by the Bradford assay (Bio-Rad Laboratories, Inc., Hercules, CA, USA). Equal quantities of proteins were separated by 12% SDS-PAGE and then transferred into the nitrocellulose membrane (Millipore Corp., Billerica, MA, USA). The membrane was blocked with 5% milk at room temperature for 1 h and then incubated with the primary antibodies for 2 h. After this step, the membrane was incubated with horseradish peroxidase-conjugated secondary antibodies (cat. no. 7072; 1:1,000; Cell Signaling Technology, Inc., Danvers, MA, USA) for 1 h at room temperature. The bands were visualized with KeyGEN Enhanced ECL detection kit (Keygen, Nanjing, China). The following antibodies used: anti-p53 (#9282, 1:1,000; Cell Signaling Technology, Inc.), anti-p21 (#2947, 1:1,000; Cell Signaling Technology, Inc.), anti-cleaved caspase 3 (#9661, 1:1,000; Cell Signaling Technology, Danvers, MA, USA), anti-cleaved caspase 8 (NB100-56116, 1:2,000; Novus Biologicals, Littleton, CO, USA), anti-cleaved caspase 9 (no. 9501, 1:2,000; Cell Signaling Technology, Inc.), anti-GAPDH mAb (3H12, 1:3,000; MBL, Nagoya, Japan).

Co-immunoprecipitation (Co-IP). The Co-IP assay was performed according to the previous publications (25). Briefly, HepG2 cells transfected with the indicated plasmids were treated with quisinostat. Cells were harvested and lysed with the NP-40 lysis buffer for 2 h at 4˚C. The cell lysates were pretreated with protein G beads for 1 h and then primary antibody was added to the supernatant and incubated overnight at 4˚C. Protein G beads were added to the lysates to pull down the immunocomplexes. The interacting proteins were detected by western blot.

Xenograft animal model. HepG2 cells were suspended with sterile PBS to make a final density of $5x10^6$ cells/ml. 200 μl of cell suspension was injected subcutaneously into the flank of the nude mice (BALB/c, 5-6 weeks of age, female) and left to grow for 2 weeks. The tumor development was checked daily. Mice were divided randomly into control group and quisinostat group. Quisinostat was given to the mice with the dosage of 2 mg/kg once daily for 15 consecutive days as previously described with minor modification (22). The control group received equal volume of 0.9% saline. The tumor volume was measured with the digital calipers and calculated with the formula (length x $width^2$)/2 (26,27). After 15 days, the mice were sacrificed by cervical dislocation. The tumor weight and mice body were also measured, respectively. This assay was approved by the Animal Research Ethics Committee of Cangzhou Central Hospital. All animals were handled following the 'Guide for the Care and Use of Laboratory Animals' and the 'Principles for the Utilization and Care of Vertebrate Animals'.

Cell cycle. HepG2 cells treated with quisinostat were washed with pre-cold PBS and then fixed in 70% ethanol. Cells were then incubated with PBS containing 40 μg/ml RNase A for 30 min at 37˚C. Followed this, cells were resuspended in PBS containing 50 μg/ml propidium iodide. The cell cycle distribution was detected by a BD FACScan Cytometer (BD Biosciences, Franklin Lakes, NJ, USA).

Generation of the p53 null HepG2 cells. The p53-null HepG2 cells was generated with the TP53-human gene knockout kit via CRISPR (KN200003; OriGene Technologies, Inc., Rockville, MD, USA) according to the manufacturer's instructions. Briefly, two targeting sequences (TCGACGCTA GGATCTGACTG; CTGTGAGTGGATCCATTGGA) were selected. To facilitate the cloning of target sequences into the pCas-Guide vector, extra bases of 'gatcg' was added to the 5'-end of the forward sequence and 'g' was added to the 3' end. Meanwhile, add 'aaaac' to the 5' end of the reverse complementary sequence and 'c' to its 3' end. The two oligos were annealed to form the double strand duplexes. The double-strand oligo DNA were ligated into the pre-cut pCAS-Guide vector according to the manufacturer's recommendation. The ligation product was transformed into the competent cells. Sequence the purified DNA to identify correct clones for proper insertion. The vector was transfected into the HepG2 cells. Positive cells harboring the vector were selected. The knockout efficiency of p53 was validated by PCR and western blot analysis.

Statistical analysis. Differences between groups were determined by Student's t-test or one way-ANOVA using the GraphPad Prism 5 (GraphPad Software, Inc., La Jolla, CA, USA). $P<0.05$ was considered to indicate a statistically

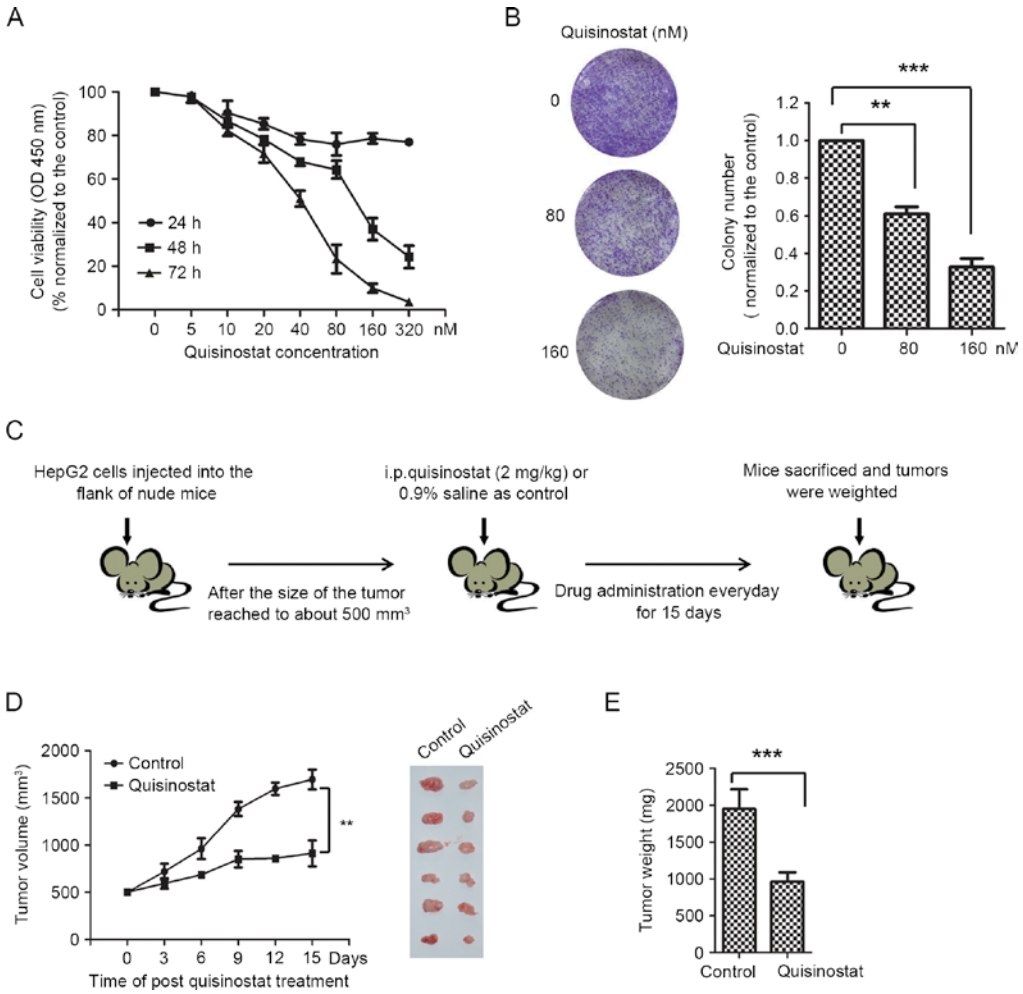

Figure 1. Quisinostat suppresses the cell growth of HepG2 cells. (A) HepG2 cells were treated with different concentrations of quisinostat for 24, 48 and 72 h. Cell viability was measured. Results are mean ± SD from three independent experiments. (B) HepG2 cells were treated with the indicated dosage of quisinostat for 48 h. The relative colony number of HepG2 cells was examined by normalizing to the cells without quisinostat treatment. **P<0.01, ***P<0.001, Student's t test. (C) The procedure of *in vivo* xenograft mice tumor model. (D and E) The tumor volume of mice subjected to quisinostat treatment and control group receiving saline was measured, respectively (left panel). (D) Mice were sacrificed after the drug administration for 15 days and the tumor were isolated (right panel). **P<0.01 (one way-ANOVA). (E) When mice were sacrificed, the tumor weight was measured. ***P<0.001 (Student's t-test).

significant difference. Data are presented as mean ± SD from three independent experiments.

Results

Quisinostat suppressed the viability of HepG2 cells. To determine the effect of quisinostat on HepG2 cell, CCK-8 assay was performed to detect the cell viability of HepG2 cell exposed to quisinostat. Cells were treated for 24, 48 and 72 h with quisinostat diluted to concentrations of 5, 10, 20, 40, 80, 160 and 320 nM. Quisinostat inhibited the viability of HepG2 cells in dose- and time-dependent manners (Fig. 1A). The IC_{50} values of cells for quisinostat treatment at 48 and 72 h were 81.2 and 30.8 nM, respectively. The growth inhibitory effect of quisinostat was also evaluated by *in vitro* colony formation assay. HepG2 cells in control group generated a number of visible colonies in 15 days, however, the number of colony formed by HepG2 cells cultured with quisinostat was significantly less than that of the control group (Fig. 1B).

To further detect the *in vivo* anti-proliferative effect of quisinostat on HCC, HepG2 cells were subcutaneously injected into the flanks of nude mice. When tumors were grown for 2 weeks, mice were treated with quisinostat for a consecutive 15 days (Fig. 1C). Significantly decreased tumor volume and tumor weight were observed with exposure of quisinostat in comparison with that of control group only receiving saline (Fig. 1D and E). In addition, no significant body weight loss was observed among mice treated with quisinostat (data not shown), suggesting no apparent toxicity of quisinostat on mice. Collectively, these results demonstrated that quisinostat has anti-proliferative effect on HepG2 cell growth.

Quisinostat promotes cell apoptosis via activation of caspase and p53 signaling. Apoptosis has been considered as a major approach to eliminate cancer cells. To detect whether the decreased cell growth induced by quisinostat was associated with the activation of cell apoptosis, HepG2 cells treated with quisinostat were subjected to FACS analysis to evaluate the cell apoptosis rate. The result showed that quisinostat treatment obviously increased the apoptosis of HepG2 cells compared with that of control cells (Fig. 2A). It has been reported that mitochondria-mediated apoptotic pathway plays

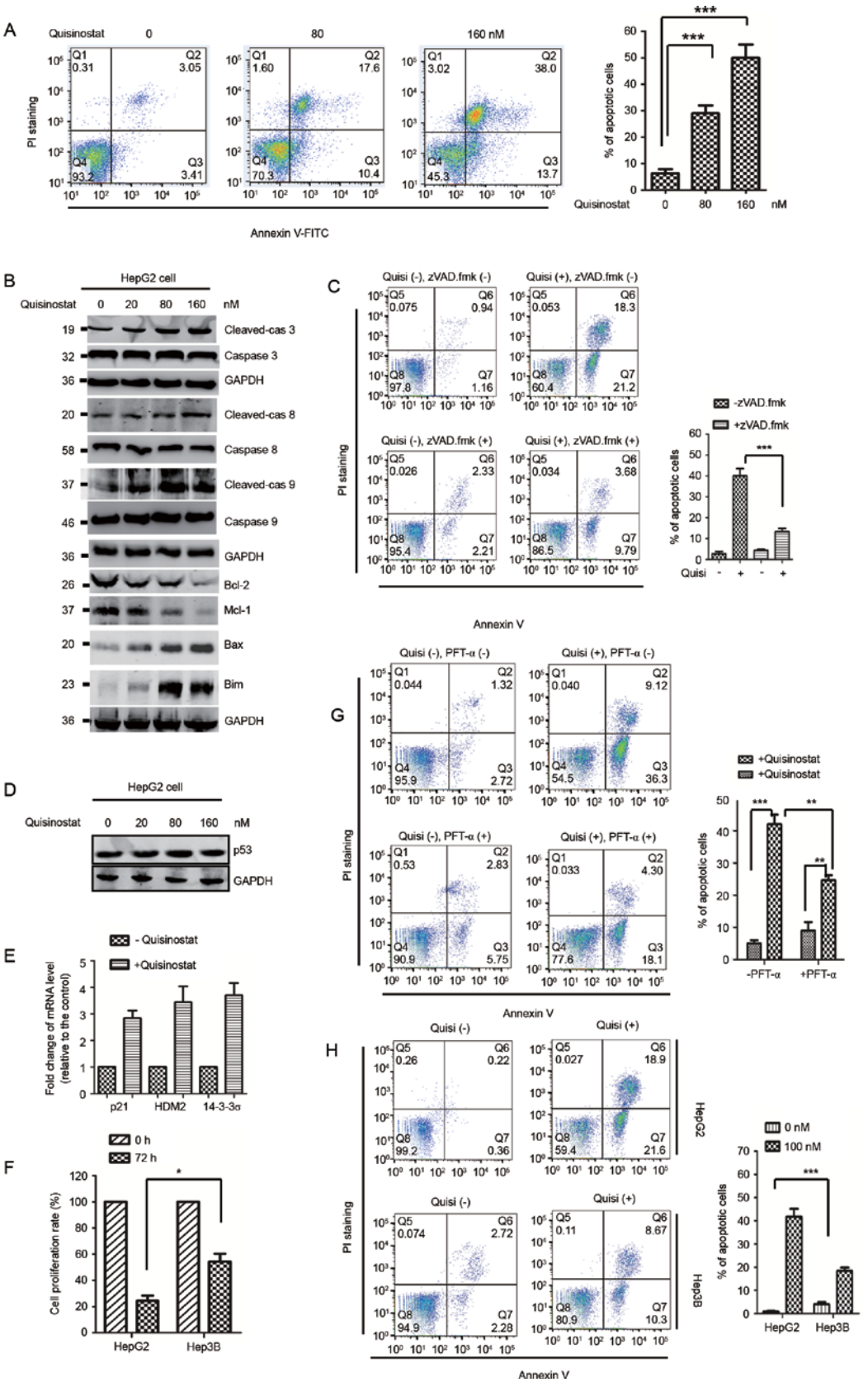

Figure 2. Quisinostat activates caspase- and p53-mediated cell apoptosis. (A) HepG2 cells were treated with the indicated dosage of quisinostat for 48 h and then the cell apoptosis rate was measured by FACS. ***P<0.001, Student's t-test. (B) HepG2 cells were exposed to quisinostat treatment and the protein abundance of Bcl-2, Mcl-1, Bim, Bax and the cleavage of caspase-3, 8, 9 were detected by western blot analysis with the indicated antibodies. (C) HepG2 cells were treated with quisinostat in the presence or absence of zVAD.fmk and the cell apoptosis was detected by flow cytometry. ***P<0.001. Student's t-test. (D) The protein level of p53 was not significantly changed with the addition of quisinostat (48 h) in HepG2 cells. (E) HepG2 cells were treated with quisinostat (80 nM) for 48 h and the mRNA level of p53 down-stream targets including p21, HDM2 and 14-3-3σ were examined by RT-PCR analysis. (F) HepG2 and Hep3B cells were treated with the quisinostat (80 nM) for 72 h. The cell proliferation rate was determined by the CCK-8 assay. *P<0.05. Student's t-test. (G) HepG2 cells were treated with quisninostat (80 nM) combination with PFT-α (30 μM) for 48 h and the cell apoptosis was detected by FACS analysis. **P<0.01, ***P<0.001, Student's t-test. (H) Cell apoptosis was performed with HepG2 and Hep3B cells treated with quisinostat for 36 h. ***P<0.001. Student's t-test.

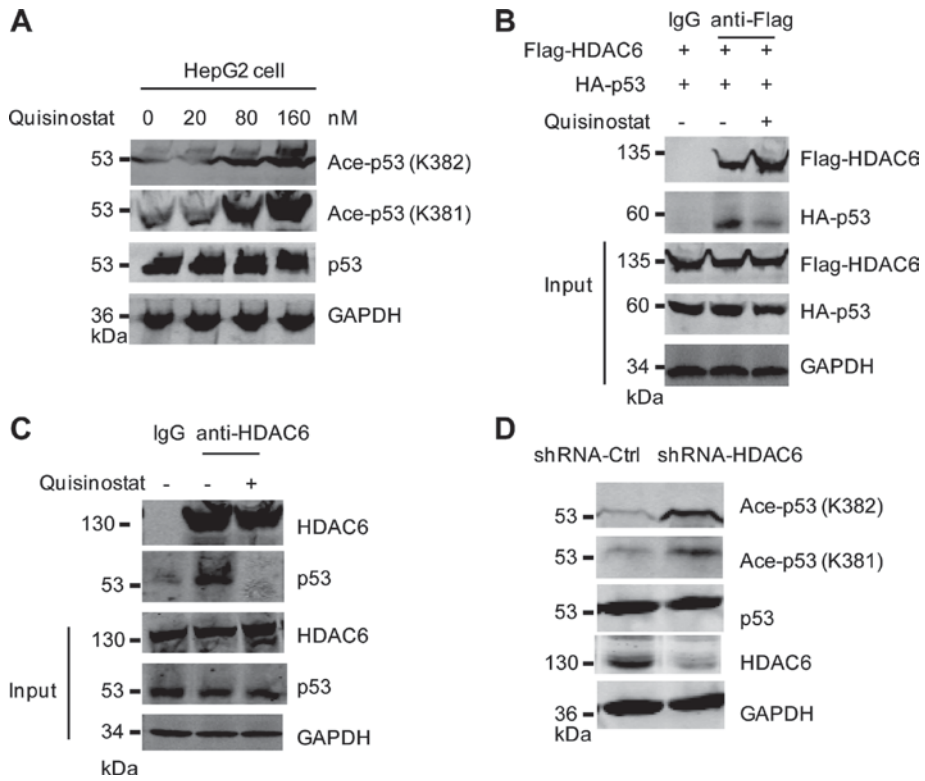

Figure 3. Quisinostat increased the acetylation of p53 via inhibiting the interaction between HDAC6 and p53. (A) HepG2 cells were treated with the quisinostat for 48 h and the level of acetylated p53 at K381/K382 was detected by western blot analysis. (B) HepG2 cells transfected with Flag-HDAC6 and HA-p53 were exposed to quisinostat (80 nM) for 36 h and the binding between HDAC6 and p53 was accessed with anti-Flag, anti-HA antibody. (C) HepG2 cells were treated with quisinostat and the endogenous binding of HDAC6 and p53 was detected. (D) HepG2 cells were transfected with shRNA-HDAC6 or shRNA- control. The expression level of acetylated p53 was measured by western blot analysis with the indicated antibodies.

important roles in inducing cell apoptosis, which releases Cyto c from the mitochondrial inner space to cytosol, and activates caspase 9 and caspase 3 via cleavage (28). To define the molecular mechanism of quisinostat-induced cell apoptosis, HepG2 cells were treated with quisinostat and the caspase activation was investigated. Western blot analysis data showed that quisinostat apparently resulted in higher expression of the cleaved caspase family proteins including caspase 8, caspase 9 and caspase 3 (Fig. 2B). Additionally, we found that HepG2 cells exposed to quisinostat exhibited a noticeably decreased expression of anti-apoptotic proteins Bcl-2 and Mcl-1 (Fig. 2B), while the abundance of pro-apoptotic protein Bax and Bim were significantly increased (Fig. 2B). To precisely determine the cell death induced by quisinostat treatment was via apoptosis, HepG2 cells were treated with quisinostat in the presence of the apoptosis inhibitor N-benzyloxycarbonyl-Val-Ala-Asp-fluoromethyl ketone (zVAD.fmk). The results showed that zVAD.fmk treatment significantly inhibited the cell apoptosis induced by quisinostat (Fig. 2C).

P53 activation is considered to be involved in apoptotic response. To detect whether quisinostat-induced cell apoptosis was also associated with p53, the expression level of p53 was detected in HepG2 cells treated with quisinostat. The protein abundance of p53 was not significantly changed with the addition of quisinostat (Fig. 2D). To determine whether quisinostat activates p53 without increasing the level of p53, the mRNA expression of p53 down-stream targets including p21, HDM2 and 14-3-3σ were evaluated by RT-PCR. The result showed that upon the treatment of quisinostat, the expression of p21, HDM2, 14-3-3σ was significantly increased (Fig. 2E), which suggested that quisinostat activates p53. To determine the contribution of p53 in quisinostat-induced HCC cell growth inhibition, HepG2 cells with wild-type p53 and Hep3B cells harboring mutated p53 were treated with quisinostat and the cell proliferation was monitored by CCK-8 assay. The result showed that upon treatment of quisinostat, significantly decreased cell proliferation was observed in HepG2 cells in comparison with that of Hep3B cells with mutated p53 (Fig. 2F). To detect the involvement of p53 in quisinostat-induced cell apoptosis, p53 inhibitor PFT-α was used to treat the cells and the cell apoptosis was measured. As shown in Fig. 2G, quisinostat treatment induced cell apoptosis, while PFT-α significantly inhibited the cell apoptosis caused by quisinostat treatment. To further determine the involvement of p53 in quisinostat induced cell apoptosis, we detected the cell apoptosis rate with Hep3B cells harboring mutated p53. Compared with that of HepG2 cells, quisinostat treatment induced a significant decreased cell apoptosis rate in Hep3B cells (Fig. 2H). These results indicated that the cell growth inhibition trigged by quisinostat is tightly associated with the activation of p53 signaling pathway.

Quisinostat increased the acetylation of p53. Acetylation is essential for the activation of p53 (29). To detect whether the activation of p53 by quisinostat treatment is associated with the acetylation status, western blot analysis was performed with HepG2 cells treated with quisinostat. The result showed that the acetylation of p53 at K381/K382 was

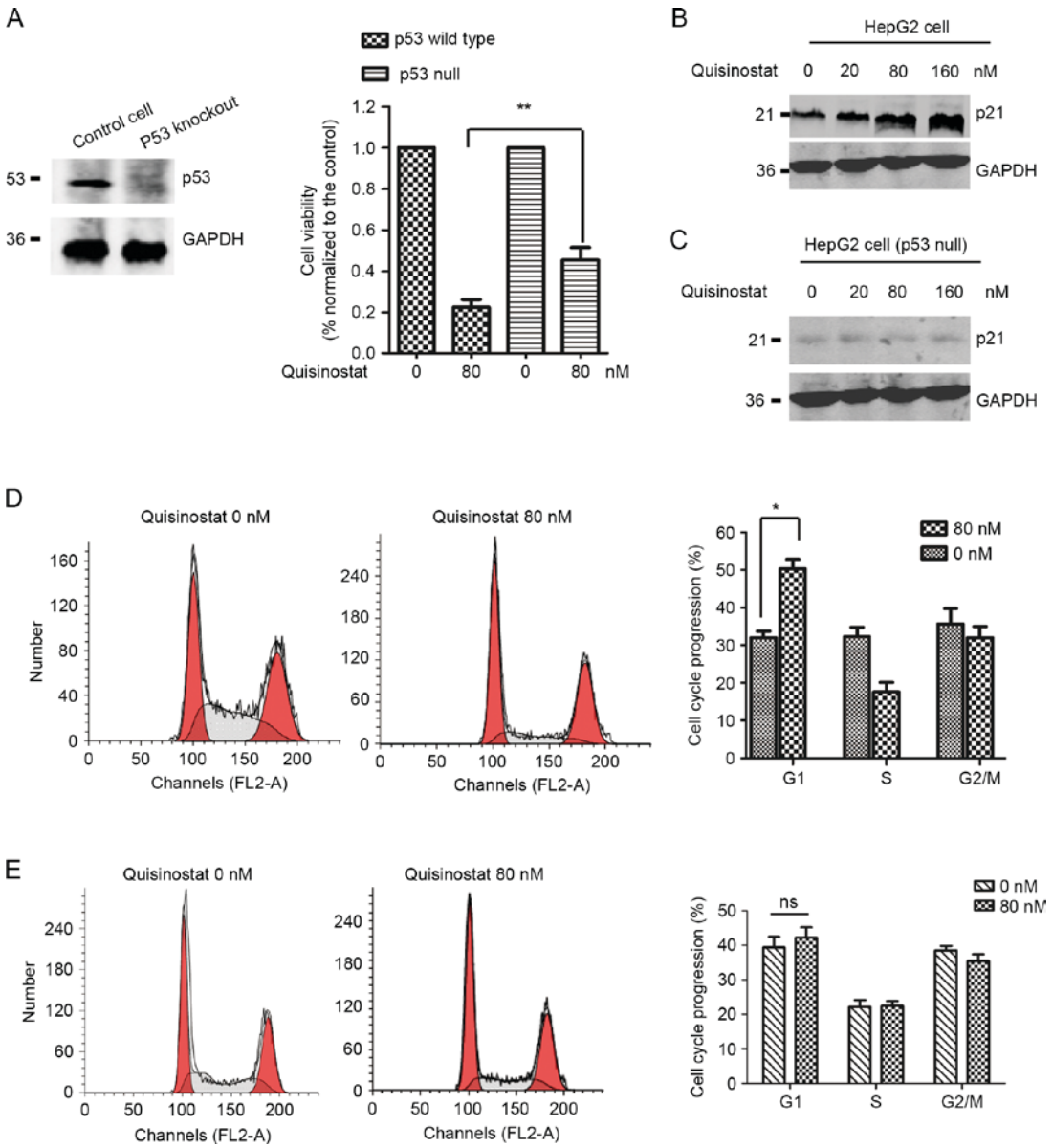

Figure 4. HepG2 cells with wild-type p53 are more sensitive to quisinostat treatment. (A) HepG2 cells with wild-type p53 or p53-null were treated with quisinostat for 72 h, and the cell viability was measured. **P<0.01, Student's t-test. The knockout efficiency of p53 was shown. (B and C) HepG2 cells harboring wild-type p53 or p53-null were treated with an increasing concentration of quisinostat for 48 h, and the protein abundance of p21 was detected by western blot analysis with anti-p21 antibody. (D) HepG2 cells were treated with quisinostat and the cell cycle distribution was detected by FACS analysis. *P<0.05, Student's t-test. (E) The cell cycle arrest induced by quisinostat treatment is tightly associated with p53. Hep3B cells with mutated p53 were treated with quisinostat and cell cycle distribution was detected by flow cytometry. Ns, not significant.

significantly increased with quisinostat treatment (Fig. 3A). Previous studies demonstrated that the histone deacetylase 6 (HDAC6) deacetylase p53 at lysine 381/382 (30,31). To further understand the molecular mechanism of the upregulated p53 acetylation induced by quisinostat, we hypothesized that addition of quisinostat may block the deacetylation of p53 by HDAC6. To determine this, we first detected the interaction between HDAC6 and p53 in the presence of quisinostat. HepG2 cells were transfected with Flag-HDAC6 and HA-p53. The Co-immunoprecipitation (Co-IP) experiment showed that the interaction between HDAC6 and p53 was weakened with the addition of quisinostat (Fig. 3B). Consistently, the endogenous binding between HDAC6 and p53 was also impaired with quisinostat treatment (Fig. 3C). To mimic the inhibitory effect of quisinostat on the binding of HDAC6 and p53, HepG2 cells were transfected with shRNA-HDAC6 to deplete the endogenous expression of HDAC6, and then the acetylation status of p53 was detected. The result showed that downregulation of HDAC6 significantly increased the acetylation of p53 at lysine 381/382 (Fig. 3D). Our data supported the conclusion that quisinostat inhibited the binding between HDAC6 and p53 and increased the acetylation of p53.

HepG2 cells with wild-type p53 are more sensitive to quisinostat treatment. Given that the activation of p53 induced by quisinostat, we determined the function of p53 in mediating the inhibitory role of quisinostat in HepG2 cells. To this end, HepG2 cells with wild-type p53 or p53-null were selected for the treatment of quisinostat, respectively. The knockout efficiency of p53 was detected by western blot analysis (Fig. 4A,

left panel). Cell viability assay suggested that quisinostat inhibited the cell viability of HepG2 cells with or without p53 (Fig. 4A, right panel). However, the inhibitory effect was much more significant in HepG2 cells with wild-type p53. This data illustrated that p53 plays important role in mediating quisinostat-induced cell growth inhibition.

To support this conclusion, we also monitored the down-stream targets of p53. The result suggested that p21, an important cell cycle regulator governing the cell progression from G1 to S phase, is significantly highly expressed in HepG2 cells with quisinostat treatment (Fig. 4B). In p53-depleted HepG2 cells, the expression level of p21 has not obviously changed (Fig. 4C). As p21 is tightly associated with cell cycle progression, we performed FACS analysis with HepG2 cells pre-treated with quisinostat. As shown in Fig. 4D, the cell cycle distribution in HepG2 cells with quisinostat treatment exhibited a significant accumulation in the G1 phase, which suggested cell cycle arrest from G1 to S phase, however, no significant cell cycle arrest was observed in p53 null HepG2 cells (Fig. 4E). There results suggested that HepG2 cells with wild-type p53 are more sensitive to quisinostat treatment.

Discussion

HCC cells display a marked resistance to currently available chemotherapeutic treatment strategies resulting in disappointing clinical outcomes in the cancer patients.

It has been recognized that epigenetic changes play important roles in the pathogenesis of a variety of human cancers (9). Therefore, alternation of epigenetic modification is identified as a novel therapeutic approach. In recent years, HDAC inhibitors have improved the treatment outcome of conventional standard chemotherapy (32-34). Among these, vorinostat (SAHA) and rimidepsin (depsipetide, FK288) have been approved by the US Food and Drug Administration (FDA) for the treatment of patients with cutaneous T cell lymphoma (35-37). Quisinostat has been reported to exhibit improved anti-proliferative activity over HDAC inhibitory compounds. Recent studies demonstrated that quisinostat inhibits the tumorigenesis of NSCLC (10,22). Notably, Heinicke U and collages demonstrated that quisinostat induced apoptosis and inhibited the growth of rhabdomyosarcoma through activating the mitochondrial pathway of apoptosis (21). This is a very interesting study, which provides novel insights into the underlying molecular mechanism of the anticancer activity of quisinostat, and more importantly, suggests the promising application of quisinostat for the treatment of rhabdomyosarcoma. This paper provides critical evidence for exploring the function of quisinostat in other types of cancers. In the present study, we showed that quisinostat suppressed the cell viability of HepG2 cells. Activation of caspase and p53 were observed in quisinostat-treated HepG2 cells. Specifically, for the activation of p53, we found that quisinostat disrupted the interaction between HDAC6 and p53, which consequently increases the acetylation of p53 and induces p53 mediated cell apoptosis.

Induction of apoptosis upon HDAC inhibitors has previously been shown in various cancers. Cell apoptosis, inducing cell death, has been a major mechanism in anti-cancer drug development. A recent study documented that quisinostat treatment in NSCLC cells increased reactive oxygen species (ROS) production and destroyed mitochondrial membrane potential, which resulting in mitochondrial-mediated cell apoptosis (10). Our results also demonstrated the activation of mitochondrial-mediated apoptotic pathway in quisinostat treated HepG2 cells. In addition, the present study demonstrated the involvement of p53 signaling in quisinostat induced cell apoptosis and growth inhibitory in HepG2 cells. Aberrantly loss-of function of p53 is critical in malignant progression of cancer cells. Increasing the expression level of wild-type p53 or activating p53 has been one of the main strategies to trigger p53-mediate physiological function, including cell apoptosis and cell cycle arrest.

Acetylation of p53 is essential for its activation (29). Upregulated p53 acetylation is involved in HDACi treatment on NSCLC cells (10). The present study found that in HepG2 cells, quisinostat increased the acetylation of p53. Recent published data demonstrated that HDAC6 catalyzed the deacetylation of p53 at lysine 381/382 (30). For the underlying mechanism, we found that addition of quisinostat disrupted the physical interaction between HDAC6 and p53, which impaired the deacelytation of p53 and increased the p53 activity. A recent study by Bao *et al* (10) showed that quisinostat treatment in NSCLC cells also resulted in the accumulation of p53 acetylation at lysine 372. Further investigation may be required to detect whether the lysine 372 acetylation of p53 is also regulated by quisinostat in HCC cells.

In summary, the present study demonstrated that quisinostat inhibited the proliferation of HepG2 cells, causing cell cycle arrest and cell apoptosis partially via upregulating the acetylation of p53 and activating caspase cleavage. Quisinostat-mediated cell growth inhibition may be helpful for HCC treatment as a potential candidate agent in clinical practice.

References

1. El-Serag HB and Rudolph KL: Hepatocellular carcinoma: Epidemiology and molecular carcinogenesis. Gastroenterology 132: 2557-2576, 2007.
2. Erichsen R, Jepsen P, Jacobsen J, Norgaard M, Vilstrup H and Sørensen HT: Time trends in incidence and prognosis of primary liver cancer and liver metastases of unknown origin in a Danish region, 1985-2004. Eur J Gastroenterol Hepatol 20: 104-110, 2008.
3. Bosch FX, Ribes J, Díaz M and Cléries R: Primary liver cancer: Worldwide incidence and trends. Gastroenterology 127 (5 Suppl 1): S5-S16, 2004.
4. Ray K: Gut microbiota: Obesity-induced microbial metabolite promotes HCC. Nat Rev Gastroenterol Hepatol 10: 442, 2013.
5. Starzl TE, Marchioro TL, Vonkaulla KN, Hermann G, Brittain RS and Waddell WR: Homotransplantation of the liver in humans. Surg Gynecol Obstet 117: 659-676, 1963.
6. Liao PH, Hsu HH, Chen TS, Chen MC, Day CH, Tu CC, Lin YM, Tsai FJ, Kuo WW and Huang CY: Phosphorylation of cofilin-1 by ERK confers HDAC inhibitor resistance in hepatocellular carcinoma cells via decreased ROS-mediated mitochondria injury. Oncogene 36: 1978-1990, 2017.
7. Ande SR, Nguyen KH, Grégoire Nyomba BL and Mishra S: Prohibitin-induced, obesity-associated insulin resistance and accompanying low-grade inflammation causes NASH and HCC. Sci Rep 6: 23608, 2016.
8. Baylin SB: Resistance, epigenetics and the cancer ecosystem. Nat Med 17: 288-289, 2011.
9. Lund AH and van Lohuizen M: Epigenetics and cancer. Genes Dev 18: 2315-2335, 2004.
10. Bao L, Diao H, Dong N, Su X, Wang B, Mo Q, Yu H, Wang X and Chen C: Histone deacetylase inhibitor induces cell apoptosis and cycle arrest in lung cancer cells via mitochondrial injury and p53 up-acetylation. Cell Biol Toxicol 32: 469-482, 2016.

11. Cui Y, Gao D, Linghu E, Zhan Q, Chen R, Brock MV, Herman JG and Guo M: Epigenetic changes and functional study of HOXA11 in human gastric cancer. Epigenomics 7: 201-213, 2015.
12. Downs B and Wang SM: Epigenetic changes in BRCA1-mutated familial breast cancer. Cancer Genet 208: 237-240, 2015.
13. Allfrey VG, Faulkner R and Mirsky AE: Acetylation and methylation of histones and their possible role in the regulation of Rna synthesis. Proc Natl Acad Sci USA 51: 786-794, 1964.
14. Kurdistani SK and Grunstein M: Histone acetylation and deacetylation in yeast. Nat Rev Mol Cell Biol 4: 276-284, 2003.
15. Yoon S and Eom GH: HDAC and HDAC inhibitor: From cancer to cardiovascular diseases. Chonnam Med J 52: 1-11, 2016.
16. Li Y and Seto E: HDACs and HDAC inhibitors in cancer development and therapy. Cold Spring Harb Perspect Med 6: pii: a026831, 2016.
17. Yang XJ and Seto E: HATs and HDACs: From structure, function and regulation to novel strategies for therapy and prevention. Oncogene 26: 5310-5318, 2007.
18. Osada H, Tatematsu Y, Saito H, Yatabe Y, Mitsudomi T and Takahashi T: Reduced expression of class II histone deacetylase genes is associated with poor prognosis in lung cancer patients. Int J Cancer 112: 26-32, 2004.
19. West AC and Johnstone RW: New and emerging HDAC inhibitors for cancer treatment. J Clin Invest 124: 30-39, 2014.
20. Kim MS, Son MW, Kim WB, In Park Y and Moon A: Apicidin, an inhibitor of histone deacetylase, prevents H-ras-induced invasive phenotype. Cancer Lett 157: 23-30, 2000.
21. Heinicke U, Kupka J, Fichter I and Fulda S: Critical role of mitochondria-mediated apoptosis for JNJ-26481585-induced antitumor activity in rhabdomyosarcoma. Oncogene 35: 3729-3741, 2016.
22. Arts J, King P, Mariën A, Floren W, Beliën A, Janssen L, Pilatte I, Roux B, Decrane L, Gilissen R, *et al*: JNJ-26481585, a novel 'second-generation' oral histone deacetylase inhibitor, shows broad-spectrum preclinical antitumoral activity. Clin Cancer Res 15: 6841-6851, 2009.
23. Cheung ST, Wong SY, Lee YT and Fan ST: GEP associates with wild-type p53 in hepatocellular carcinoma. Oncol Rep 15: 1507-1511, 2006.
24. Dai Q, Yin Y, Liu W, Wei L, Zhou Y, Li Z, You Q, Lu N and Guo Q: Two p53-related metabolic regulators, TIGAR and SCO2, contribute to oroxylin A-mediated glucose metabolism in human hepatoma HepG2 cells. Int J Biochem Cell Biol 45: 1468-1478, 2013.
25. Zhang CZ, Chen GG, Merchant JL and Lai PB: Interaction between ZBP-89 and p53 mutants and its contribution to effects of HDACi on hepatocellular carcinoma. Cell Cycle 11: 322-334, 2012.
26. Laporte AN, Barrott JJ, Yao RJ, Poulin NM, Brodin BA, Jones KB, Underhill TM and Nielsen TO: HDAC and proteasome inhibitors synergize to activate pro-apoptotic factors in synovial sarcoma. PLoS One 12: e0169407: 2017.
27. Faustino-Rocha A, Oliveira PA, Pinho-Oliveira J, Teixeira-Guedes C, Soares-Maia R, da Costa RG, Colaço B, Pires MJ, Colaço J, Ferreira R and Ginja M: Estimation of rat mammary tumor volume using caliper and ultrasonography measurements. Lab Anim (NY) 42: 217-224, 2013.
28. Green DR: Apoptotic pathways: Ten minutes to dead. Cell 121: 671-674, 2005.
29. Tang Y, Zhao W, Chen Y, Zhao Y and Gu W: Acetylation is indispensable for p53 activation. Cell 133: 612-626, 2008.
30. Ryu HW, Shin DH, Lee DH, Choi J, Han G, Lee KY and Kwon SH: HDAC6 deacetylates p53 at lysines 381/382 and differentially coordinates p53-induced apoptosis. Cancer Lett 391: 162-171, 2017.
31. Ding G, Liu HD, Huang Q, Liang HX, Ding ZH, Liao ZJ and Huang G: HDAC6 promotes hepatocellular carcinoma progression by inhibiting P53 transcriptional activity. FEBS Lett 587: 880-886, 2013.
32. Mariadason JM: HDACs and HDAC inhibitors in colon cancer. Epigenetics 3: 28-37, 2008.
33. Pelicci PG: A new class of anti-cancer drugs: HDAC-inhibitors. Suppl Tumori 1: S66, 2002.
34. Secrist JP, Zhou X and Richon VM: HDAC inhibitors for the treatment of cancer. Curr Opin Investig Drugs 4: 1422-1427, 2003.
35. Duvic M and Vu J: Vorinostat in cutaneous T-cell lymphoma. Drugs Today (Barc) 43: 585-599, 2007.
36. Duvic M and Vu J: Vorinostat: A new oral histone deacetylase inhibitor approved for cutaneous T-cell lymphoma. Expert Opin Investig Drugs 16: 1111-1120, 2007.
37. Murata M, Towatari M, Kosugi H, Tanimoto M, Ueda R, Saito H and Naoe T: Apoptotic cytotoxic effects of a histone deacetylase inhibitor, FK228, on malignant lymphoid cells. Jpn J Cancer Res 91: 1154-1160, 2000.